 CMES, vol.63, no.1, pp.79-100, 2010

Accurate True Direction Solutions to the Euler Equations Using a Uniform Distribution Equilibrium Method

Alex Ferguson[1], **Matthew R. Smith**[2] **and J.-S. Wu**[3]

Abstract: A novel approach for the use of multiple continuous uniform distributions for reconstruction of the Maxwell-Boltzmann equilibrium probability distribution function is used for the solution of one and two dimensional Euler equations. The Uniform distribution Equilibrium Flux Method (UEFM) is a kinetic-theory based flux solver which calculates true directional, volume to volume fluxes based on integration (over velocity space and physical space) of a sum of uniform probability distribution functions working to approximate the equilibrium distribution function. The resulting flux expressions contain only the Heaviside unit step function and do not require the evaluation of the Exponential or Error Functions. The proposed method is verified using a series of one and two dimensional benchmarks and is shown to provide a higher level of accuracy (for a given computational expense) when compared to the similar Quiet Direct Simulation (QDS) method.

Keywords: Kinetic Theory of Gases, Euler Equations, Computational Fluid Dynamics, CFD.

1 Introduction

Conventional Finite Volume Methods (FVMs) represent a general method for obtaining the numerical solution to a set of governing Partial Differential Equations. These equations, in conservation form, possess fluxion gradients which are traditionally discretized using the divergence theorem. The numerical method is performed through calculation of direction decoupled fluxes across the finite volume surfaces, or cell interfaces, which provide an estimate of the flux gradient and thus the rate of change of conserved quantities in each finite volume, often called a cell. The disadvantage to this conventional approach is that flux exchange is not con-

[1] State Operations, Kellogg Brown & Root Pty. Ltd., Australia.
[2] National Center for High-performance Computing, HsinChu, Taiwan.
[3] National Chiao Tung University, Department of Mechanical Engineering, HsinChu, Taiwan. Corresponding author: chongsin@faculty.nctu.edu.tw

ducted in a physically realistic fashion. The solution requires direction decoupling at cell surfaces [Smith, Macrossan and Abdel-jawad (2008); Smith, Macrossan, Cave and Wu (2009)] traditionally employing a series of one-dimensional fluxes at cell interfaces rather than a true directional flux. Another consequence is that flux exchange is only permitted between cells sharing an adjacent interface, which is not consistent with reality, since gas molecules are permitted to move in any direction. These disadvantages lead to errors in the numerical solution when the flow direction is not aligned with the computational grid [Smith, Macrossan and Abdel-jawad (2008); Smith, Macrossan, Cave and Wu (2009)]. These errors can be substantial and while the use of multi-step methods helps to alleviate error, it does not remove it completely.

An alternative approach was first proposed by Bird (1994) in the Direct Simulation Monte Carlo (DSMC) method. The underlying assumption of the DSMC method is that flow may be separated into two phases – a movement phase, where particles move in free-flight over a small time step, and a collision phase, where molecular interactions result in an exchange of momentum and energy between regions. During the free-flight movement phase, fluxes of mass, momentum and energy are carried by particles whose velocities are implicitly determined from a local velocity distribution function. In the limit of thermal equilibrium, the velocity probability distribution function is the Maxwell-Boltzmann equilibrium velocity probability distribution function. The Equilibrium Particle Simulation Method (EPSM) was thus proposed by Pullin (1980) as an equilibrium alternative to the DSMC method where particles are assigned velocities from the equilibrium velocity distribution function during the collision phase rather than conducting collisions directly, which can greatly reduce the computational time.

At the same time, Pullin (1980) proposed a "continuum equivalent" to the EPSM method, which he called the Equilibrium Flux Method (EFM). The fluxes of mass, momentum and energy across the surfaces of the cells were calculated by taking moments of the Maxwell-Boltzmann equilibrium probability distribution function. However, EFM also suffers from the errors introduced from direction decoupling when the flow is not well aligned with computational grid. Later, Smith et. al. proposed a general form of the method known as the True Direction Equilibrium Flux Method (TDEFM). Fluxes calculated by TDEFM represent the true analytical solution to the molecular free flight problem under the assumption of thermal equilibrium and uniformly distributed quantities [Smith, Macrossan and Abdel-jawad (2008); Smith, Macrossan, Cave and Wu (2009)]. However, despite being accurate, the method is often portrayed as prohibitively expensive to compute and thus its application to scientific computation is limited.

Albright, Daughton, Lemons, Winske, and Jones (2002) and Albright, Lemons,

Jones, and Winske (2002) previously developed a numerical scheme for the solution of the Euler Equations known as the Quiet Direct Simulation Monte Carlo (QDSMC). In this method, the integrals encountered in the TDEFM formulation are replaced by approximations – using Gaussian numerical integration – effectively replacing the continuous velocity distribution function with a series of discrete velocities. The method was later extended to higher order spatial accuracy by Smith et.al. and renamed as the Quiet Direct Simulation (QDS) method due to the lack of stochastic processes [Smith. Cave, Wu, Jermy, and Chen (2009), Cave, Smith, Wu, Jermy, Krumdieck and Tseng (2010)]. The lack of complex mathematical functions results in a computationally efficient scheme with a performance higher than that of EFM while maintaining the advantages of true directional fluxes. This computational efficiency came at the cost of accuracy with a slow rate of convergence towards the analytical solution provided by TDEFM, which will be shown later in this study.

Presented here is a novel, true direction numerical scheme called the Uniform distribution Equilibrium Flux Method (UEFM). Rather than employing a set of discrete velocities to approximate the velocity probability distribution function, UEFM fluxes are calculated from a cumulative series of continuous, uniform velocity probability distribution functions approximating the equilibrium distribution function. The resulting flux expressions contain only the Heaviside unit step function and do not require the evaluation of the Exponential or Error Functions – resulting in a numerical scheme with a higher accuracy than that of QDS while maintaining a high level of computational efficiency. The proposed method is verified using a series of one and two dimensional benchmarks which demonstrate these attributes.

2 True Direction Equilibrium Flux Method (TDEFM)

Since the proposed UEFM is strongly related to TDEFM, which is a method for calculation of true direction volume-to-volume fluxes, the TDEFM is briefly described here for reference. The fluxes obtained using TDEFM represent the analytical solution to molecular motion under the assumptions of (i) thermal equilibrium, (ii) uniform conditions across any given finite volume, and (iii) molecular free flight. The TDEFM fluxes also represent the QDS result in the limit of an infinite number of discrete velocities and also the proposed UEFM result in the limit of an infinite number of uniform velocity distributions. Full details of the TDEFM derivation can be found in [Smith, Macrossan and Abdel-jawad (2008)] while the one dimensional mass fluxes are covered here briefly. The probability of a particle possessing

a velocity v between v_1 and v_2 is

$$p(v1 \leq x \leq v2) = \int_{v1}^{v1} g(v)dv \tag{1}$$

where g(v) is the Maxwell-Boltzmann equilibrium velocity probability distribution function;

$$g(v) = \frac{1}{\sqrt{2\pi}s} \exp\left[\frac{-(v-\bar{v})^2}{2s^2}\right] \tag{2}$$

where s is the variance of the equilibrium velocity distribution $s = \sqrt{RT}$. The probability of a particle at location x being able to move in molecular free flight to a region between x_l and x_r is (refer to Figure 1 for definitions of x_l and x_r) during time Δt is:

$$p(x) = \int_{\frac{x_l - x}{\Delta t}}^{\frac{x_r - x}{\Delta t}} g(v)dv \tag{3}$$

The average probability of particles from a source region between x_L and x_R (refer to Figure 1 for definitions of x_L and x_R) moving into the specified destination region is

$$\bar{p}(x_L, x_R, x_l, x_r) = \frac{1}{x_R - x_L} \int_{x_L}^{x_R} p(x)dx. \tag{4}$$

Multiplication of this by the mass in the source region provides the net mass flux to successfully move from the source region to the destination region:

$$\begin{aligned} M =& \rho V \cdot \bar{p}(xL, xR, xl, xr) \\ =& M_C \exp\left[\frac{-(x_R - x_l + \bar{v}\Delta t)^2}{2\sigma^2\Delta t^2}\right] + M_1 erf\left[\frac{x_R - x_l + \bar{v}\Delta t}{\sqrt{2}\sigma\Delta t}\right] \\ & - M_C \exp\left[\frac{-(x_R - x_r + \bar{v}\Delta t)^2}{2\sigma^2\Delta t^2}\right] - M_2 erf\left[\frac{x_R - x_r + \bar{v}\Delta t}{\sqrt{2}\sigma\Delta t}\right] \\ & - M_C \exp\left[\frac{-(x_L - x_l + \bar{v}\Delta t)^2}{2\sigma^2\Delta t^2}\right] - M_3 erf\left[\frac{x_L - x_l + \bar{v}\Delta t}{\sqrt{2}\sigma\Delta t}\right] \\ & + M_C \exp\left[\frac{-(x_L - x_r + \bar{v}\Delta t)^2}{2\sigma^2\Delta t^2}\right] + M_4 erf\left[\frac{x_L - x_r + \bar{v}\Delta t}{\sqrt{2}\sigma\Delta t}\right] \end{aligned} \tag{5}$$

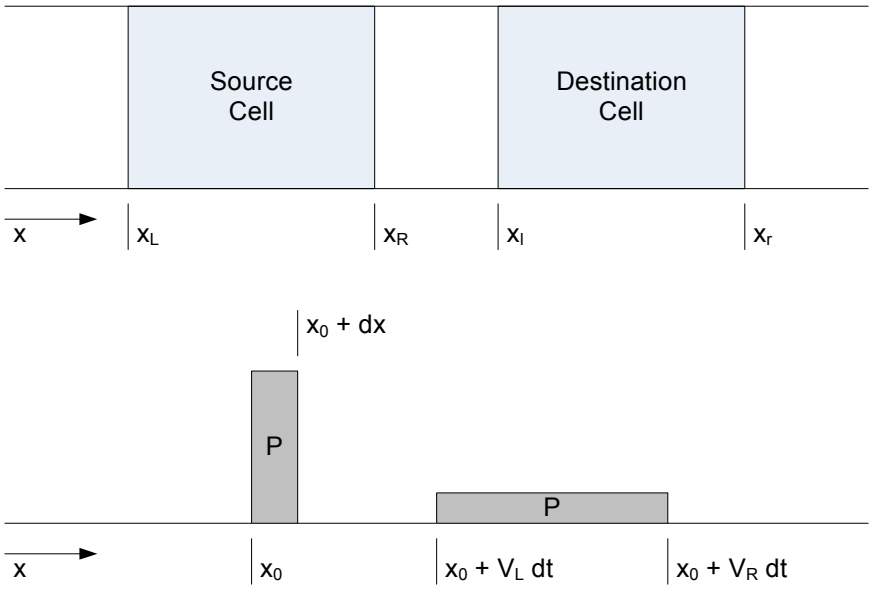

Figure 1: (Top) Typical (1D) Cell arrangement. (Bottom) Redistribution of Conserved Quantities for a given uniform Velocity Distribution (V_L to V_R).

where M_C, M_1, M_2, M_3 and M_4 are constants defined in [Smith, Macrossan and Abdel-jawad (2008)] and as follows:

$$\begin{aligned}
M_C &= \frac{s\Delta t}{(x_R - x_L)\sqrt{2\pi}} \\
M_1 &= \frac{1}{2(x_R - x_L)}(\bar{v}\Delta t - x_l + x_R) \\
M_2 &= \frac{1}{2(x_R - x_L)}(\bar{v}\Delta t - x_r + x_R) \\
M_3 &= \frac{1}{2(x_R - x_L)}(\bar{v}\Delta t - x_l + x_L) \\
M_4 &= \frac{1}{2(x_R - x_L)}(\bar{v}\Delta t - x_r + x_L)
\end{aligned} \tag{6}$$

The resulting expression contains a large number of error and exponential functions (erf(x) and exp(x) respectively) which result in large computational expense when evaluated. More details regarding derivation of fluxes of momentum and energy can be found in [Smith, Macrossan and Abdel-jawad (2008)]. The important concept is multiple integrations of the probability distribution function are required in predict-

ing a volume-to-volume flux. Conventional kinetic theory-based flux solvers (such as EFM [Pullin (1980)]) employ single moments over velocity space to calculate the flux across a single specific point (or surface, in higher dimensions).

3 Uniform Distribution Equilibrium Flux Method

The proposed Uniform distribution Equilibrium Flux Method (UEFM) avoids the computational expense associated with TDEFM while maintaining its true-direction nature. This is accomplished by discretization of a Gaussian (normal) distribution function (representing the distribution of molecular speeds in a gas at equilibrium) by the sequential summation of uniform distribution functions (shown in Figure 2). A uniform distribution function is one that, for $V_L \leq v \leq V_R$, the function takes on a constant value (and zero elsewhere) such that:

$$\int_{-\infty}^{\infty} f(v)\,dv = 1.$$

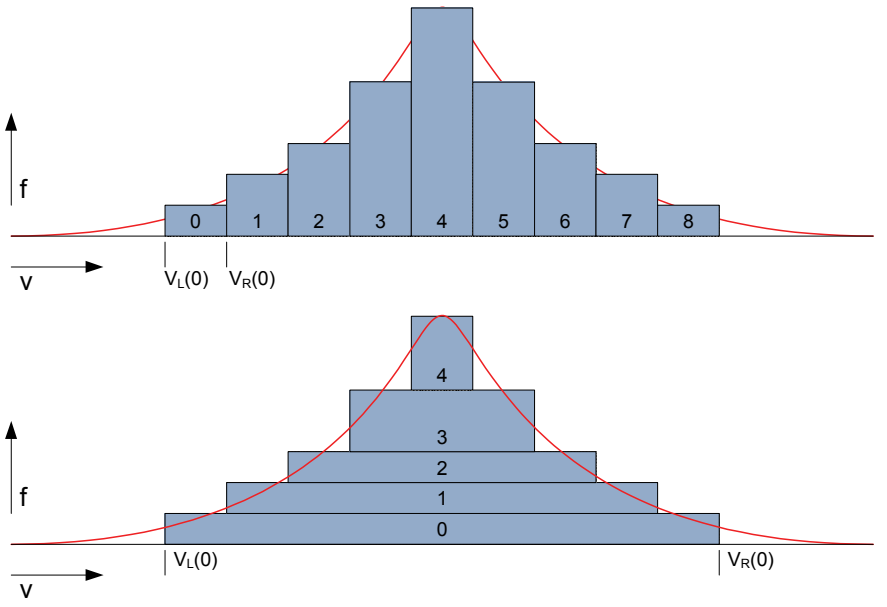

Figure 2: Discretization of the Maxwell-Boltzman Equilibrium (Normal) Distribution Function. (Top) the Binomial Distribution Fit, and (Bottom) The Re-cast binomial distribution.

The selection of appropriate weights and velocity limits is such that the local (i.e. within a given source region) mass, momentum and energy is conserved.

3.1 Flux Expressions

Presented is the detailed derivation of the mass, momentum and energy flux calculated using the proposed UEFM method. Particles located at position x_0, having equal probability of a velocity within the range (V_L, V_R) and moving in free-flight over time Δt will be distributed evenly within the physical range $x_0 + V_L \Delta t$ and $x_0 + V_R \Delta t$ (as previously shown in Figure 1). The re-distribution of mass (per unit source mass) having moved for a period Δt is:

$$G(x_0, x, V_L, V_R, \Delta t) = \frac{1}{(V_R - V_L)\Delta t}\left[H(x0, x, V_L) - H(x0, x, V_R)\right] \tag{7}$$

where $H(x0, x, V) = H[-x0 + x - V\Delta t]$ is the Heaviside unit step function:

$$H(x) = \begin{cases} 0, & x < 0 \\ 1, & x \geq 0 \end{cases} \tag{8}$$

It is important to note that $H(x)$ is dimensionless. The function G represents a spatial probability distribution function describing how particles are distributed over space x from starting location x_0. Taking the moment of G around x_0 over the width of the source region provides the source cell average value of G, written as $\bar{G}_{MASS}$ with units of (m-1):

$$\begin{aligned} &\bar{G}_{MASS} \\ =&\frac{1}{(x_R - x_L)} \int_{x_L}^{x_R} G dx_0 \\ =&\frac{1}{(V_L - V_R)(x_R - x_L)\Delta t} \\ &+ H[-\Delta t V_L + x_{xL}]\left((x_L - x_R) H[-\Delta t V_L + x_{xR}] + (\Delta t V_L - x_{xL}) H[\Delta t V_L - x_{xR}]\right) \\ &- H[-\Delta t V_R + x_{xL}]\left((x_L - x_R) H[-\Delta t V_R + x_{xL}] + (\Delta t V_R - x_{xL}) H[\Delta t V_R - x_{xR}]\right) \end{aligned} \tag{9}$$

Where $x_{xL} = x - x_L$, $x_{xR} = x - x_R$.

The integral of this over all possible values of x returns unity – meaning that all mass must land in some finite destination region. This function is shown in Figure 3 for various values of V_L, V_R and Δt. The net flux of mass (per unit source mass)

from the source region between x_L and x_R and destination region between x and $x+\Delta x$ is given by $F_{MASS} = \bar{G}_{MASS}\Delta x$. Complete integration of this expression (with respect to destination location x) across a destination region (x_l, x_r) then gives the total flux of mass (per unit source mass) from the source to the destination region:

$$\begin{aligned}
&F_{MASS}(x_l, x_r, x_L, x_R, V_L, V_R) \\
=&\int_{x_l}^{x_r} \bar{G}_{MASS} dx \\
=&\frac{1}{2\Delta t\,(x_L - x_R)\,(V_L - V_R)} \\
&\Big((\Delta t V_L - x_l + x_L)^2 H[-\Delta t V_L + x_l - x_L] - (\Delta t V_R - x_l + x_L)^2 H[-\Delta t V_R + x_l - x_L] \\
&- (\Delta t V_L - x_r + x_L)^2 H[-\Delta t V_L + x_r - x_L] + (\Delta t V_R - x_r + x_L)^2 H[-\Delta t V_R + x_r - x_L] \\
&- (\Delta t V_L - x_l + x_R)^2 H[-\Delta t V_L + x_l - x_R] + (\Delta t V_R - x_l + x_R)^2 H[-\Delta t V_R + x_l - x_R] \\
&+ (\Delta t V_L - x_r + x_R)^2 H[-\Delta t V_L + x_r - x_R] - (\Delta t V_R - x_r + x_R)^2 H[-\Delta t V_R + x_r - x_R] \Big)
\end{aligned} \tag{10}$$

The average momentum (per unit source mass) carried by particles having the same distribution G from a source region $x_L \le x \le x_R$is found by taking the moment:

$$\begin{aligned}
\bar{G}_{MOM} =& \frac{1}{(x_R - x_L)} \int_{x_L}^{x_R} \left(\frac{x - x_0}{\Delta t} \right) G dx_0 \\
=& \frac{1}{2\,(V_L - V_R)\,(x_R - x_L)\,\Delta t^2} \\
&\Big\{ + H[-\Delta t V_L + x - x_L] \,(\, (x_L - x_R)\,(2x - x_L - x_R)\, H[-\Delta t V_L + x - x_R] \\
&- (\Delta t V_L + x - x_L)\,(\Delta t V_L - x + x_L)\, H[-\Delta t V_L + x - x_R] \,) \\
&- H[-\Delta t V_R + x - x_L] \,(\, (x_L - x_R)\,(2x - x_L - x_R)\, H[-\Delta t V_R + x - x_R] \\
&- (\Delta t V_R + x - x_L)\,(\Delta t V_R - x + x_L)\, H[-\Delta t V_R + x - x_R] \Big\}
\end{aligned} \tag{11}$$

This function is shown graphed in Figure 4, with units of (s^{-1}). The integral of $\bar{G}_{MOM}$ over any region now provides the net momentum per unit source (or, in other words, the average "particle" velocity) to fall into the region integrated. Specifically, integration of $\bar{G}_{MOM}$ across the source region $x_l \le x \le x_r$provides the general

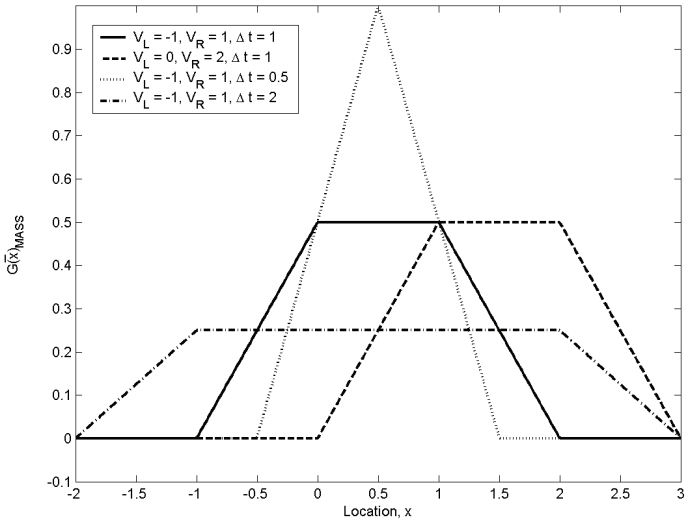

Figure 3: Average $G(x)$ (over source region between 0 and 1) plotted over -2 < x < 3. Regardless of variable values, the integral over all possible values must be unity.

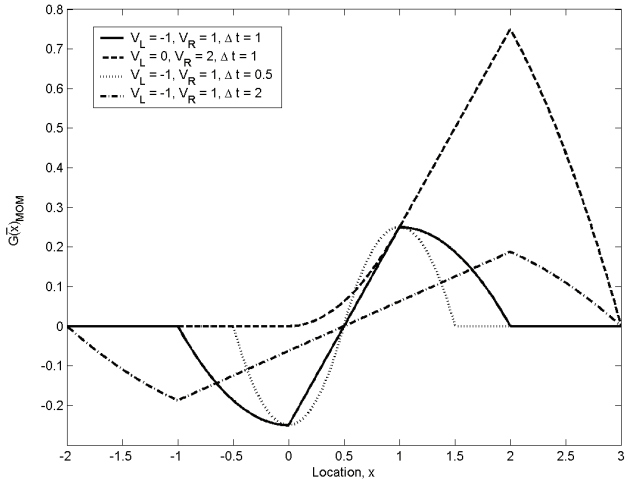

Figure 4: Moment of velocity taken over $G(x)$ (over source region between 0 and 1) plotted over -2 < x < 3. Regardless of variable values, the integral over all possible values must be equal to the total momentum in the source region (per unit source mass).

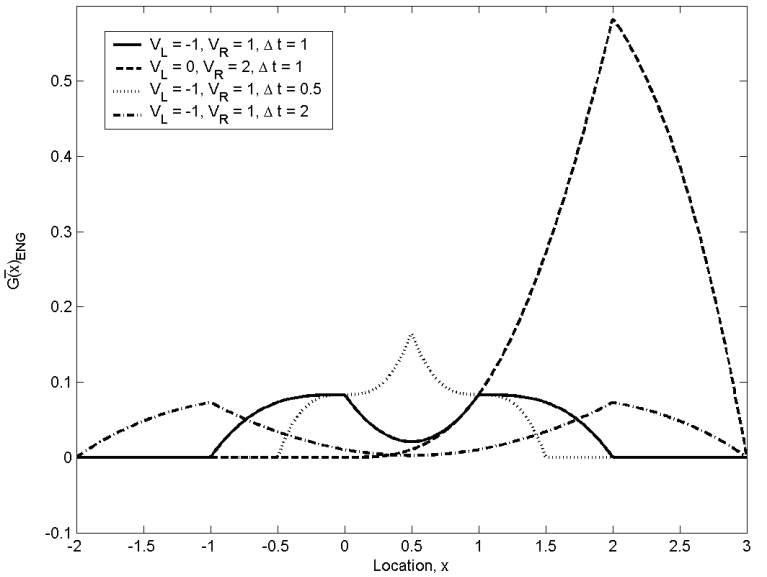

Figure 5: Moment of energy taken over G (over source region between 0 and 1) plotted over -2 < x < 3. Regardless of variable values, the integral over all possible values must be equal to the total momentum in the source region (per unit source mass).

expression for the momentum flux (per unit source mass):

$$
\begin{aligned}
&F_{MOM}\left(x_l,x_r,x_L,x_R,V_L,V_R\right)\\
&=\int_{x_l}^{x_r}\bar{G}_{MOM}dx\\
&=\frac{1}{6\left(x_L-x_R\right)\left(V_R-V_L\right)\Delta t^2}\\
&\Big(+\left(2\Delta tV_L+x_l-x_L\right)\left(\Delta tV_L-x_l+x_L\right)^2H\left[-\Delta tV_L+x_l-x_L\right]\\
&-\left(2\Delta tV_R+x_l-x_L\right)\left(\Delta tV_R-x_l+x_L\right)^2H\left[-\Delta tV_R+x_l-x_L\right]\\
&-\left(2\Delta tV_L+x_r-x_L\right)\left(\Delta tV_L-x_r+x_L\right)^2H\left[-\Delta tV_L+x_r-x_L\right]\\
&+\left(2\Delta tV_R+x_r-x_L\right)\left(\Delta tV_R-x_r+x_L\right)^2H\left[-\Delta tV_R+x_r-x_L\right]\\
&-\left(2\Delta tV_L+x_l-x_R\right)\left(\Delta tV_L-x_l+x_R\right)^2H\left[-\Delta tV_L+x_l-x_R\right]\\
&+\left(2\Delta tV_R+x_l-x_R\right)\left(\Delta tV_R-x_l+x_R\right)^2H\left[-\Delta tV_R+x_l-x_R\right]\\
&+\left(2\Delta tV_L+x_r-x_R\right)\left(\Delta tV_L-x_r+x_R\right)^2H\left[-\Delta tV_L+x_r-x_R\right]\\
&-\left(2\Delta tV_R+x_r-x_R\right)\left(\Delta tV_R-x_r+x_R\right)^2H\left[-\Delta tV_R+x_r-x_R\right]\Big)
\end{aligned}
\tag{12}
$$

Particles located at position x_0 moving for some time Δt take with them energy (per unit source mass) described by:

$$E = \left(\frac{1}{2} \left(\frac{x - x_0}{\Delta t} \right)^2 + C \right) \tag{13}$$

where C is the internal energy and thermal energy associated with unused translational degrees of freedom. The expression for the average evolution of energy ($\bar{G}_{ENG}$, with units of ms^{-2}) is also found by taking a moment of the energy around G:

$$\begin{aligned}
\bar{G}_{ENG} =& \frac{1}{(x_R - x_L)} \int_{x_L}^{x_R} EG dx_0 \\
=& \frac{H\left[-\Delta t V_L + x - x_L\right]}{6\left(V_L - V_R\right)\left(x_R - x_L\right)\Delta t^3} \\
& \Big\{ \left(x_L - x_R\right)\left(6C\Delta t^2 + 3x^2 + x_L^2 + x_L x_R + x_R^2 - 3x\left(x_L + x_R\right)\right) H \\
& \left[-\Delta t V_L + x - x_R\right] \\
& - \left(\Delta t V_L + x - x_L\right)\left(6C\Delta t^2 + \Delta t^2 V_L^2 + \Delta t V_L\left(x - x_L\right) + \left(x - x_L\right)^2\right) H \\
& \left[-\Delta t V_L + x - x_R\right] \Big\} \\
& - \frac{H\left[-\Delta t V_R + x - x_L\right]}{6\left(V_L - V_R\right)\left(x_R - x_L\right)\Delta t^3} \\
& \Big\{ \left(x_L - x_R\right)\left(6C\Delta t^2 + 3x^2 + x_L^2 + x_L x_R + x_R^2 - 3x\left(x_L + x_R\right)\right) H \\
& \left[-\Delta t V_R + x - x_R\right] \\
& - \left(\Delta t V_R + x - x_L\right)\left(6C\Delta t^2 + \Delta t^2 V_R^2 + \Delta t V_R\left(x - x_L\right) + \left(x - x_L\right)^2\right) H \\
& \left[-\Delta t V_R + x - x_R\right] \Big\}
\end{aligned} \tag{14}$$

This function is shown (for various values of V_L, V_R and Δt) in Figure 5. The integral bound by all possible destination regions (-∞,∞) must be equal to the energy contained (per unit mass) within the source region. Following the mass and momentum flux derivation, integration of $\bar{G}_{ENG}$across the source region $x_l \leq x \leq x_r$

provides the general expression for the energy flux (per unit source mass):

$$
\begin{aligned}
&F_{ENG}\left(x_l,x_r,x_L,x_R,V_L,V_R\right)\\
=&\int_{x_l}^{x_r}\bar{G}_{ENG}dx\\
=&\frac{1}{24\left(x_L-x_R\right)\left(V_R-V_L\right)\Delta t^3}\\
&\Big(+\left(A+2\Delta t^2V_L^2+\Delta t^2V_L^2+2\Delta tV_Lx_{lL}+x_{lL}^2\right)\left(\Delta tV_L-x_{lL}\right)^2H\left[-\Delta tV_L+x_{lL}\right]\\
&-\left(A+2\Delta t^2V_R^2+\Delta t^2V_R^2+2\Delta tV_Rx_{lL}+x_{lL}^2\right)\left(\Delta tV_R-x_{lL}\right)^2H\left[-\Delta tV_R+x_{lL}\right]\\
&-\left(A+2\Delta t^2V_L^2+\Delta t^2V_L^2+2\Delta tV_Lx_{rL}+x_{rL}^2\right)\left(\Delta tV_L-x_{rL}\right)^2H\left[-\Delta tV_L+x_{rL}\right]\\
&+\left(A+2\Delta t^2V_R^2+\Delta t^2V_R^2+2\Delta tV_Rx_{rL}+x_{rL}^2\right)\left(\Delta tV_R-x_{rL}\right)^2H\left[-\Delta tV_R+x_{rL}\right]\\
&-\left(A+2\Delta t^2V_L^2+\Delta t^2V_L^2+2\Delta tV_Lx_{lR}+x_{lR}^2\right)\left(\Delta tV_L-x_{lR}\right)^2H\left[-\Delta tV_L+x_{lR}\right]\\
&+\left(A+2\Delta t^2V_R^2+\Delta t^2V_R^2+2\Delta tV_Rx_{lR}+x_{lR}^2\right)\left(\Delta tV_R-x_{lR}\right)^2H\left[-\Delta tV_R+x_{lR}\right]\\
&+\left(A+2\Delta t^2V_L^2+\Delta t^2V_L^2+2\Delta tV_Lx_{rR}+x_{rR}^2\right)\left(\Delta tV_L-x_{rR}\right)^2H\left[-\Delta tV_L+x_{rR}\right]\\
&-\left(A+2\Delta t^2V_R^2+\Delta t^2V_R^2+2\Delta tV_Rx_{rR}+x_{rR}^2\right)\left(\Delta tV_R-x_{rR}\right)^2H\left[-\Delta tV_R+x_{rR}\right]\Big)
\end{aligned}
\tag{15}
$$

where: $x_{lL}=x_l-x_L$, $x_{rL}=x_r-x_L$, $x_{rR}=x_r-x_R$, $x_{lR}=x_l-x_R$, and $A=12C\Delta t^2$.

3.2 Distribution Scaling and Conservation

Thus far, the flux expressions have been developed to only consider a single uniform distribution function. In either case where (i) a single distribution or (ii) a series of uniform distribution functions are employed, the variance and mean of the summed distributions must be equal to that of the original governing equilibrium distribution. For the single uniform distribution (one 'particle' or 'bucket') case, this is trivial. For multiple (summed) distributions, any number of approaches is possible: however, since the normal distribution is the limiting case of the binomial distribution, it is natural to choose this discrete probability distribution as the basis for our discretization scheme when multiple buckets are employed:

$$
P_p\left(n|N\right)=\frac{N!}{n!\left(N-n\right)!}p^n\left(1-p\right)^{(N-n)} \tag{16}
$$

where $N!/n!\left(N-n\right)!$ is the usual binomial coefficient. The binomial distribution has a mean of Np and variance of $Np\left(1-p\right)$. The location of the abissca is then translated to achieve a zero mean and subsequently scaled to match their combined variance with that of the equilibrium (normal) distribution in each cell (Figure 2). The weights are also evaluated and then re-scaled to ensure that the total area under

the curve is unity (i.e. conservation of mass). The total flux of mass, momentum and energy (per unit source mass) is thus calculated from the cumulative sum of these velocity bands;

$$\begin{aligned} F_{MASS\_TOTAL} &= \sum_{i=1}^{N} W_i F_{MASS}(x_l, x_r, x_L, x_R, V_{Li}, V_{Ri}) \\ F_{MOM\_TOTAL} &= \sum_{i=1}^{N} W_i F_{MOM}(x_l, x_r, x_L, x_R, V_{Li}, V_{Ri}) \\ F_{ENG\_TOTAL} &= \sum_{i=1}^{N} W_i F_{ENG}(x_l, x_r, x_L, x_R, V_{Li}, V_{Ri}) \end{aligned} \tag{17}$$

3.3 Discrete Mass versus Discrete Velocity

The proposed UEFM method is similar to the previously developed QDS method with the major exception being the style of discretization. While the QDS method employs a set of discrete velocities with varying masses, the proposed UEFM method employs a set of discrete masses (or more accurately, discrete probability densities) across continuous velocity space. This has several advantages over QDS, primarily being computational efficiency and accuracy. Greater accuracy results since a complete range of velocities is included in the flux calculations; discrete velocities such as those used by QDS result in errors in the predicted thermal (diffusive) fluxes which become important where flows are diffusion dominated. A simple flux test is employed to gauge and compare the error in flux predicted by both the QDS and UEFM schemes. Progressive increase of the number of velocity buckets employed in both QDS and UEFM are used in flux calculation and compared with the TDEFM flux to gauge their respective convergence rates. The test, described in Figure 6, involves calculation of the mass flux moving into a diagonally adjacent neighbour and comparison to the analytical solution taken from TDEFM. The error is calculated by taking the L2 normalised error of the two results, i.e.

$$L2_{UEFM} = \sqrt{\frac{(\rho_{UEFM} - \rho_{TDEFM})^2}{\rho_{TDEFM}^2}} \tag{18}$$

The results plotted in Figure 6 demonstrate that the UEFM algorithm performs better with fewer discretizations and converges towards the TDEFM result faster than the QDS result. For reference, the set of scaled velocity bounds V_L and V_R (together with the weighting for each distribution) employed for a varying number of discretizations is shown in Table 1.

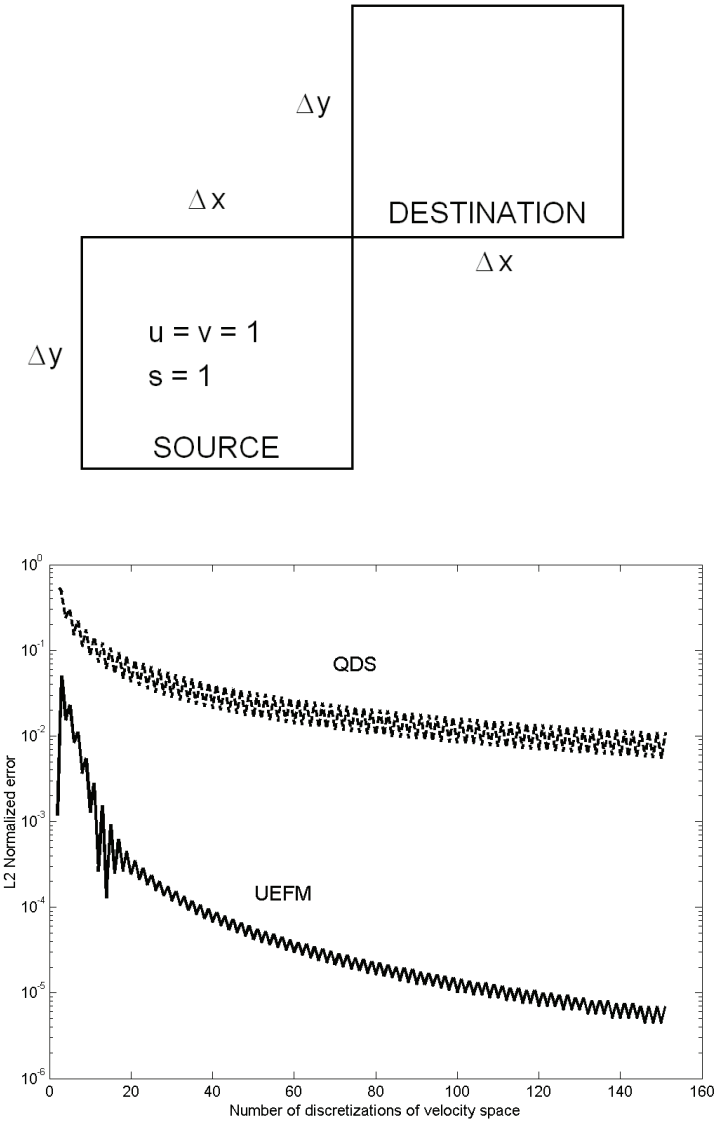

Figure 6: (Top) Geometry of flux test with source cell allowing molecular free flight to a destination cell. The cell width and height are both unity. (bottom) The L2 normalised error for QDS and UEFM as a function of the number of discretizations representing the Maxwell-Boltzman equilibrium distribution.

Table 1: Sample scaled velocities and weights for the UEFM scheme taken from the binomial distribution for the test problem demonstrated in Figure 6.

Discretizations	Scaled Velocities V_L and V_R	Weights W
2	$(V_L,V_R)_1$ = (-2.10618, +2.10618)	W_1=0.635825
	$(V_L,V_R)_2$ = (-0.702059, +0.702059)	W_2=0.364175
3	$(V_L,V_R)_1$ = (-2.4905, +2.4905)	W_1=0.272443
	$(V_L,V_R)_2$ = (-1.4943, +1.4943)	W_2=0.569138
	$(V_L,V_R)_3$ = (-0.4981, +0.4981)	W_3=0.158419
4	$(V_L,V_R)_1$ = (-2.82613, +2.82613)	W_1=0.113898
	$(V_L,V_R)_2$ = (-2.01866, +2.01866)	W_2=0.349382
	$(V_L,V_R)_3$ = (-1.2112, +1.2122)	W_3=0.444078
	$(V_L,V_R)_4$ = (-0.403733, +0.403733)	W_4=0.0926419

4 Results and Discussion

4.1 Sod's 1D Shock Tube

UEFM is applied to Sod's 1D Shock Tube problem to benchmark its performance against both QDS and TDEFM. A perfect ideal gas ($\gamma = 1.4$) fills a region between $0 \leq x \leq L$ with an imaginary diaphragm separates gases of different conditions located at $x = 0.5L$. The initial conditions are:

$$\rho(x) = \begin{cases} 10, & x \leq \frac{L}{2} \\ 1, & x > \frac{L}{2} \end{cases} \quad T(x) = 1.0 \quad u(x) = 0.0$$

At $t = 0$, the fictitious diaphragm is removed and the simulation is progressed to a dimensionless time of $0.1L/(RT)^{0.5}$. A constant kinetic CFL of 0.5 is enforced. It should be noted that selection of this CFL number has no relation to the stability of the method but is only necessary to limit the flux of conserved quantities from one cell to an immediately adjacent neighbour. Figure 7 shows the results of the various simulation methods employed. The shock structure and expansion fan are clearly evident and closely matches the expected result as predicted by TDEFM. The error, predicted through comparison to the TDEFM solution, as a function of location along the shock tube is plotted in Figure 8. Results demonstrates that, although both methods demonstrate significant errors within the shock region (approximately 1% for both QDS and UEFM), the maximum error in the resolution of the contact surface and expansion is highly reduced.

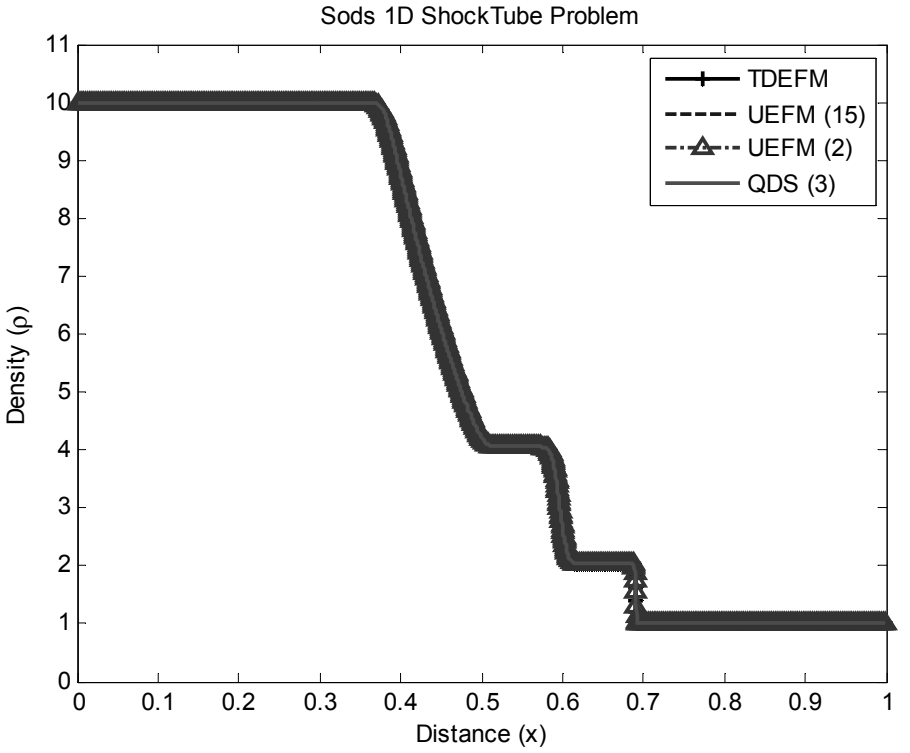

Figure 7: Results of the 1D Sods Shock Tube Problem for various solvers. A 1D region of length L initially contains two gases at rest separated by an imaginary diaphragm at L = 0.5. The density and temperature ratio across the diaphragm is 10 and 1 respectively. Numbers in brackets indicate the number of buckets used to approximate the Equilibrium Distribution. Results are presented for 2000 cells at dimensionless time of 0.1.

4.2 Two Dimensional Blast Wave

To test the various errors of UEFM and QDS and their symptoms, UEFM, QDS and TDEFM are individually applied to the simulation of a two dimensional blast wave. The problem consists of an ideal inviscid gas ($\gamma = 1.4$) at rest with a circular region of radius r holding a temperature 100 times that of the surrounding gas. The simulation is conducted on a 200x200 grid and is allowed to proceed to a dimensionless time of 0.025 with the kinetic CFL limited to 0.5. Plots of the simulation output recast in radial coordinates (Figure 9) demonstrates the true-direction nature of the UEFM result, which is again, notably closer to the TDEFM result than the QDS

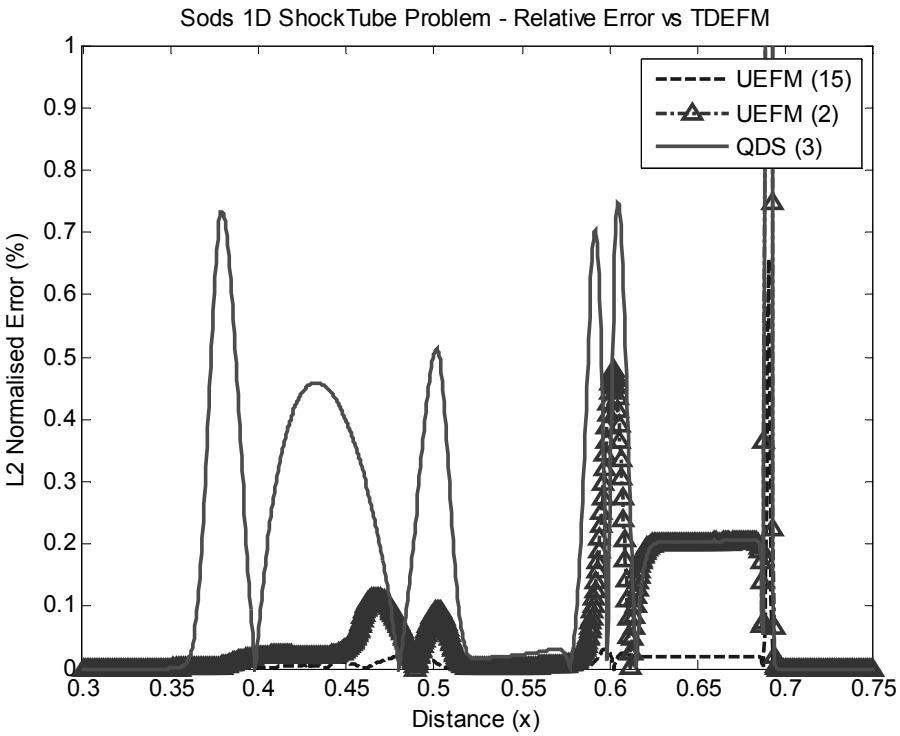

Figure 8: The L2 Normalised Error in the results of the 1D sods Shock Tube for various solvers. Error is calculated through comparison against the TDEFM solution. Numbers in Brackets indicate the number of buckets used to approximate the Equilibrium Distribution.

simulation. Radial symmetry is well captured by the scheme. Figure 10 plots the L2 error for both UEFM and QDS (as compared with TDEFM) and demonstrates a tenfold increase in the accuracy of the UEFM representation with a computational expense of similar magnitude.

4.3 Supersonic flow over a cylinder

UEFM is applied to an inviscid, ideal (γ=1) high speed flow with a non-aligned grid and its results compared against the solution provided by TDEFM and QDS. The problem is that of a cylindrical tube placed perpendicular to a flow with a free-stream velocity of Mach 3. The flow-field of dimensions length L and height H= 3L is discretized by a Cartesian mesh of 1200x400 cells. The cylinder ($r^2 = 0.125H^2$) is approximated by this mesh and centred on x = L/2.4, y= 0, where y= 0

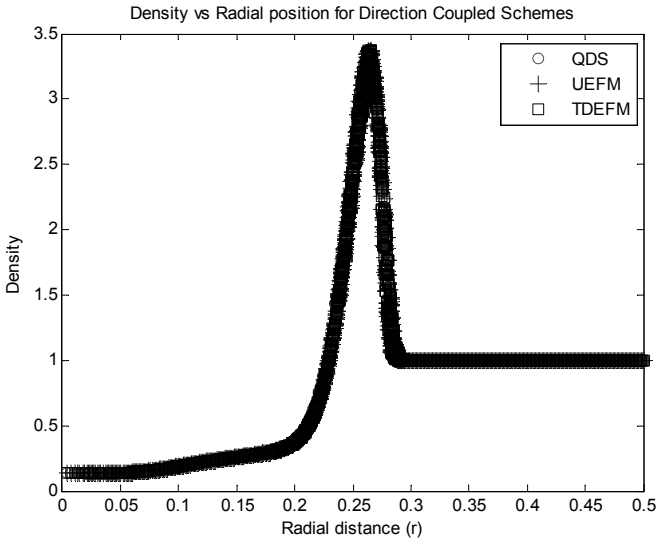

(a)

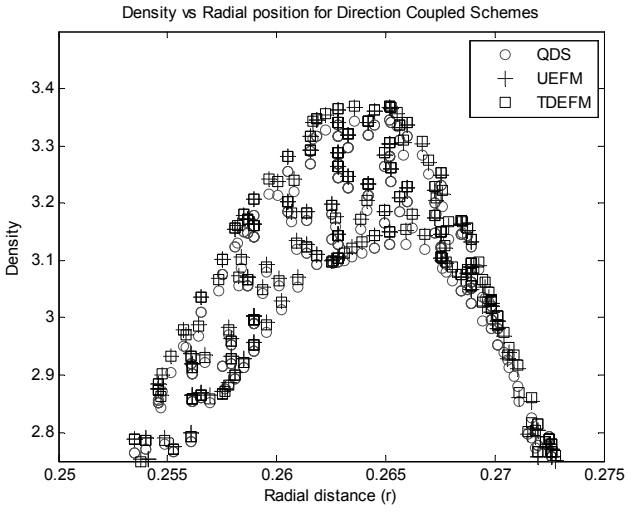

(b)

Figure 9: a - Results of the two-dimensional blast wave simulation. Density plotted against radial distance from the blast centre. A circular region of gas with a density and temperature of 1 and 100 times that of the surrounding gas is allowed to expand until dimensionless time 0.025; b - Results of the two-dimensional blast wave simulation. An enlarged view of the region between ($0.25 < r < 0.275$) in Figure 9a showing alignment of the UEFM and TDEFM results.

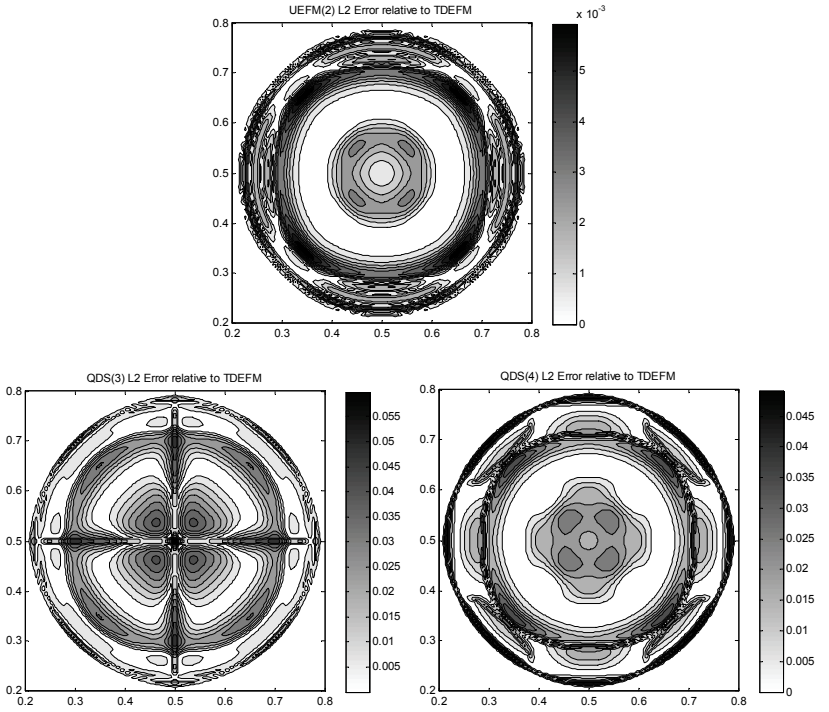

Figure 10: L2 error as compared with the TDEFM result for the two dimensional blast problem. (Top) UEFM, (Bottom left) QDS employing 3 particles per direction, and (Bottom right) QDS employing 4 particles per direction.

also describes an axis of symmetry. The simulation was advanced in an unsteady time stepping procedure until a steady solution was obtained. The results of the simulation are plotted in Figure 11 to Figure 14. Comparing QDS and UEFM to the TDEFM result, again UEFM is shown to attain greater accuracy even at low resolutions. Problems with resolution of stagnation regions, present in the QDS solution, are absent in the UEFM solution. Minor errors in shock structures are present for both the QDS and UEFM solution.

5 Conclusion

A novel approach for the use of multiple continuous uniform distributions for reconstruction of the Maxwell-Boltzmann equilibrium probability distribution function has been used for the solution of one and two dimensional Euler equations. The Uniform distribution Equilibrium Flux Method (UEFM) is a kinetic-theory based

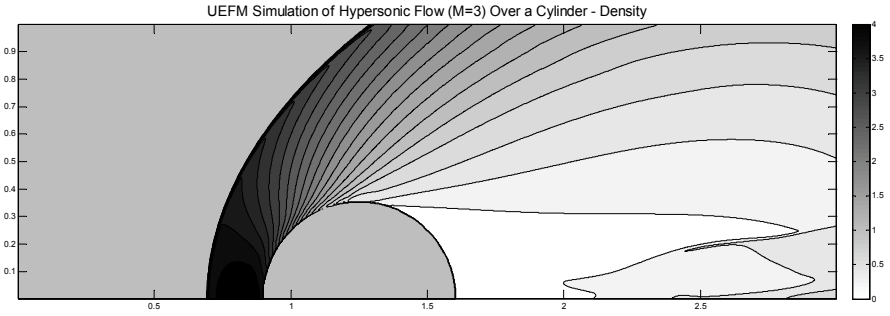

Figure 11: Density contours taken from the UEFM Simulation of Hypersonic Flow (M=3) Over a Cylinder. All surfaces (With exception to the inflow and outflow) are slip surfaces (i.e. flow is inviscid) while outflow boundaries employed conditions interpolated from interior cells.

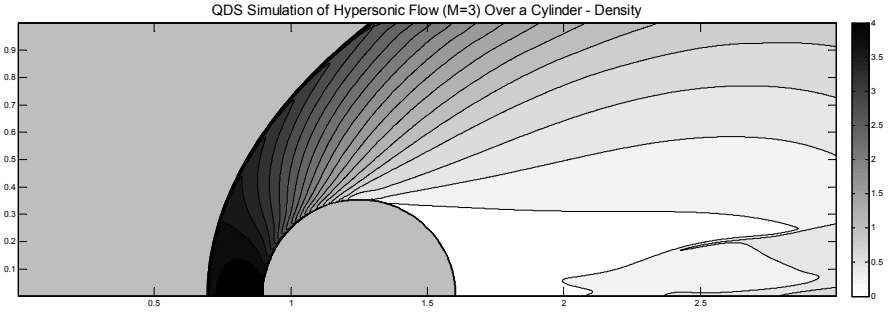

Figure 12: Density contours taken from the UEFM Simulation of Hypersonic Flow (M=3) Over a Cylinder. All surfaces (With exception to the inflow and outflow) are slip surfaces (i.e. flow is inviscid) while outflow boundaries employed conditions interpolated from interior cells.

flux solver which calculates true directional, volume to volume fluxes based on integration (over velocity space and physical space) of a sum of uniform probability distribution functions working to approximate the equilibrium distribution function. The resulting flux expressions contain only the Heaviside unit step function and do not require the evaluation of the Exponential or Error Functions. The proposed method has been verified by a series of one and two dimensional benchmarks and is shown to provide a higher level of accuracy (for a given computational expense) when compared to the similar Quiet Direct Simulation (QDS) method. The

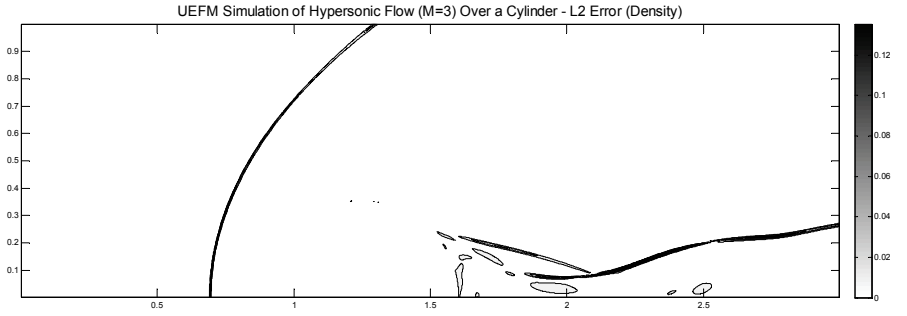

Figure 13: L2 error in Density of the UEFM simulation calculated through comparison with TDEFM.

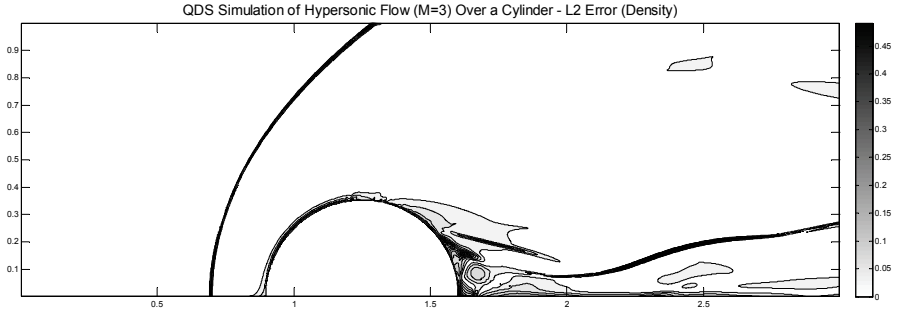

Figure 14: L2 error in density of the QDS simulation calculated through comparison with TDEFM.

method is shown to quickly converge to the TDEFM result which it approximates; maintaining all the advantages of its true-direction nature.

References

Albright, B. J.; Daughton, W.; Lemons, D.S.; Winske, D.; Jones, M.E. (2002):Quiet direct simulation of Plasmas, *Physics of Plasmas*, 9, pp. 1898.

Albright, B. J.; Lemons, D.S.; Jones, M.E.; Winske, D. (2002): *Quiet direct simulation of Eulerian fluids*, *Physical Review E*, 65 (055302): pp.1-4.

Bird, G.A. (1994): *Molecular Gas Dynamics and the Direct Simulation of Gas Flows*, Oxford University Press, 1994.

Cave, H.M.; Smith, M.R.; Wu, J.-S.; Jermy, M.C.; Krumdieck, S.P.; Tseng,

K.-C. (2010): Axisymmetric Simulations of Eulerian Gas Flows using the Quiet Direct Simulation Method, submitted to *AIAA Journal*, February 2010.

Pullin, D.I. (1980): 'Direct simulation methods for compressible ideal gas flow, *Journal of Computational Physics*, 34: pp. 231-144.

Smith. M.R.; Cave, H.M.; Wu, J.-S.; Jermy, M.C.; Chen, Y.-S. (2009): An improved Quiet Direct Simulation method for Eulerian fluids using a second-order scheme, *Journal of Computational Physics*, 228(6): pp. 2213-2224.

Smith. M.R.; Macrossan, M.N.; Abdel-jawad, M.M. (2008): Effects of Direction Decoupling in Flux Calculation in Euler Solvers, *Journal of Computational Physics*, 227(8): pp. 4142-4161.

Smith, M.R.; Macrossan, M.N.; Cave, H.M.; Wu, J.-S. (2009): *An Approximate Method for Solving Rarefied and Transitional Flows Using TDEFM with Isotropic Mesh Adaptation*, Rarefied Gas Dynamics (AIP Conference Proceedings) (Ed. Takashi, A.) American Institute of Physics.